

98-249



Environment
Canada

Environnement
Canada

Canada



NATIONAL WATER
RESEARCH INSTITUTE
INSTITUT NATIONAL DE
RECHERCHE SUR LES EAUX

TD
226
N87
No. 98-
249

Groundwater Flow in a Fractured Carbonate
Aquifer Inferred from Combined Hydro-
geological and Geochemical Measurements
BY

L. Zanini, K. Novakowski, P. Lapcevic

NWRI Contribution No. 98-249

MANAGEMENT PERSPECTIVE

Title: Groundwater flow in a Fractured Carbonate Aquifer Inferred from Combined Hydrogeological and Geochemical Measurements

Author(s): L. Zanini, K. Novakowski, P. Lapcevic, G. Bickerton, J. Voralek and C. Talbot

NWRI Publication No.: 98-249

Citation:

EC Priority/Issue:

During the late 1970's and early 1980's a PCB waste management site was operating on the outskirts of the town of Smithville, located approximately 15 km south of Lake Ontario, on the Niagara escarpment. In 1985, it was discovered that PCB oils and associated solvents had penetrated the into the ground and pervaded the upper horizons of the bedrock underlying the site. This resulted in the closure of a local water supply which utilized groundwater from this aquifer. An ongoing investigation into the extent of groundwater contamination is currently underway.

A fraction of the PCBs and associated contaminants can migrate with the groundwater along the groundwater flow path. Thus, a conceptual model of the groundwater flow system is needed before any interpretation of contaminant migration with the groundwater is attempted. This study involves detailed analyses of the physical and inorganic chemical properties of both the fractured bedrock and groundwater at the site. By combining these data, a conceptual model of the groundwater flow system can be delineated. Such a model can be used in future numerical simulations that will provide valuable insight into the fate and transport of groundwater contaminants at the site.

This works supports EC priorities on Ecosystem Health and Ecosystem Initiatives under COA Stream 1.4 (contaminated sites) and Stream 1.6 (groundwater).

Current Status:

The report was submitted to the journal of Ground Water for publication.

Next Steps:

This study is currently completed and the objectives fulfilled. However, the results presented in the report will be used to aid future studies and develop a numerical model.

Groundwater Flow in a Fractured Carbonate Aquifer Inferred from Combined Hydrogeological and Geochemical Measurements

For submission to: Ground Water Sept 21/98

L. Zanini, K.S. Novakowski, P. Lapcevic, G.S. Bickerton, J. Voralek and C. Talbot

National Water Research Institute, 867 Lakeshore Rd., Burlington, Ontario, N2J 3B7
Canada

Contact: Dr. Kent Novakowski, Dept. of Earth Science, Brock University, 500 Glenridge Ave.,
St. Catharines, Ontario, L2S 3A1, Canada
phone: (905) 688-5550 X3859
e-mail: Kent@craton.geol.brocku.ca

ABSTRACT

A conceptual model for regional groundwater flow is presented for a fractured Silurian dolomite in the Niagara Escarpment area of Southern Ontario. Both physical and chemical hydrogeological observations obtained from field investigations are used to deduce the structure of the groundwater flow system in the fracture network. The field study was conducted using six boreholes drilled in the vicinity of the town of Smithville. The boreholes were diamond cored through the entire thickness of the dolomite formation (approximately 45 m), hydraulically tested using a 2 m packer spacing and then completed using multi-packer casing strings. Measurements of hydraulic head were obtained on a weekly basis over a period of two years, and geochemical analyses for inorganic and isotopic analyses were collected from each borehole interval. Transmissivity measurements indicate that the dolomite is divided into two groundwater flow systems separated by an extensive unit of low transmissivity throughout the region. The upper flow system is characterized by water enriched in Mg and SO_4 . Below the low transmissivity zone, groundwater increases in salinity, and is enriched in Ca and SO_4 . Based on the geochemistry, the rate of groundwater migration in the lower flow system is surmised to be less than that in the upper system. Measurements of hydraulic head in conjunction with

the results of the analyses of the environmental isotopes ($\delta^{18}\text{O}$ and $\delta^2\text{H}$) suggest that groundwater flow is mainly horizontal and likely governed by enlarged bedding plane fractures. The isotope geochemistry and topographical features further suggests that groundwater recharge is occurring approximately 2 km to the north of Smithville.

INTRODUCTION

The Niagara Escarpment is an extensive geological structure that extends along the western shoreline of Lake Ontario (Fig.1). This feature is comprised of a stratigraphic sequence of dolostone and shale units that includes the Lockport Formation as the cap rock (Tesmer, 1981). The Lockport Formation is an important source of water for many of the farming communities in the Niagara region. It also underlies numerous industrialized cities and towns. As a result, chlorinated solvents have contaminated the groundwater at several locations (Masalia and Johnson, 1984, Yager et al., 1997).

During the late 1970's and early 1980's a PCB management site was operated on the outskirts of the town of Smithville, located approximately 15 km south of Lake Ontario, on the Niagara escarpment (Fig.1). In 1985, it was discovered that PCB oils and associated solvents had penetrated the overburden and pervaded the upper horizons of the Lockport Formation. This resulted in the closure of a local water supply which utilized groundwater from this aquifer.

In order to develop a remedial strategy for the site, a conceptual model for regional groundwater flow and contaminant transport in the bedrock is required. The primary purpose of this study is to use both physical and geochemical hydrogeological observations in the construction of such a conceptual model. Physical hydrogeological observations include measurement of the distribution of transmissivity and measurement of hydraulic head at selected depth intervals in the Lockport Formation. Geochemical observations include measurements of the inorganic ionic content, stable

isotopic ($\delta^{18}\text{O}$, δD) and tritium (^3H) composition of the groundwater, as well as determination of the chemical composition of the rock units. Inorganic ion concentration of the groundwater is used in conjunction with hydraulic measurements to determine preferential flow paths in the fracture network. Trends in the concentrations of dissolved inorganic ions are used to define differing groundwater flow regimes and isotopic composition is used as an indicator of groundwater recharge. Thus, the geochemical data provides information on the groundwater flow system that can not be deduced using hydraulic information alone. Recent application of this approach was used to develop a conceptual groundwater flow model for granitic rock in Aspö, Sweden (Smellie et al., 1995) and for the fractured Chalk aquifer in the United Kingdom (Hiscock et al., 1996).

SITE GEOLOGY AND HYDROGEOLOGY

The PCB contaminated site is located just north of the town of Smithville, Ontario (Figure 1). The surface topography (Figure 1) indicates the presence of a swale oriented in the east-west direction, located approximately 1.5 km to the north of the site and a river (20 mile creek) flowing from the north-west to the south-east, located approximately 1 km to the south of the site. The topographical gradient in the vicinity of the site, is relatively flat with a slight inclination of approximately 10 m/km south. Approximately 5 to 10 m of clay till overburden underlies the site (Figure 2). The clay till is of minimal permeability ($K \sim 10^{-9}$ to 10^{-11} m/s) although pervaded by sparse vertical fractures some of which may be fully penetrating (Golders Associates, 1995). The Lockport Formation underlying the clay till is comprised of four geological members consisting of fine to medium grained dolostone that dip in a southeasterly direction at an angle of 0.5° (Golders Associates, 1995). The upper member (Eramosa) of the Lockport Formation is 10 to 20 m in thickness and is fractured in a relatively uniform manner. Transmissivity of the of the fractures can be

as high as 10^{-2} m²/s (Golders Associates, 1995). The Vinemount member, which underlies the Eramosa, is characterized by a weathered vuggy zone (1 to 4 m thick) and a zone of unfractured rock of relatively low transmissivity (3 to 4 m in thickness). The lower members (Goat Island and Gasport) are 6 to 7 m and 8 to 10 m in thickness respectively. Fracture frequency in these units is more sparse, although transmissivity is no less than that observed in the Eramosa member. The Lockport Formation is underlain by an impermeable shale of up to 17 m in thickness and is considered a regional aquitard (Golders Associates, 1995).

Groundwater flow in the fracture system is generally to the southeast, following stratigraphic dip of the geological units (Golders Associates, 1995). Based on the previous studies of the Lockport Formation conducted at this site and elsewhere in the region, it is inferred that groundwater flow is primarily governed by bedding plane fractures that are laterally extensive and have limited vertical interconnection (Novakowski and Lapcevic, 1988; Riechart, 1990; Golders Associates, 1995). Thus, it is assumed that groundwater flow in the Lockport Formation underlying the contaminated site is primarily in the horizontal direction, carried by bedding plane fractures of unknown lateral extent and unknown vertical interconnectivity. Previous site investigations (Golders Associates, 1995) indicate that some fractures, at least in the upper Lockport members, are observed to be laterally connected over a distance of 1 km as evidenced by the downgradient transport of aqueous-phase contamination emanating from the PCB source. Hydraulic gradients in this zone have been estimated to be 0.02 with initial estimates of groundwater velocity ranging 20 - 6000 m/a whereas hydraulic gradients in some of the lower dolostone members are estimated at values ranging from 0.001 to 0.007 (Golders Associates, 1995). Groundwater flow in localized areas may vary depending on the nature of the fracture system. The resulting variations in hydraulic gradient are subtle and therefore may be inadequate to identify fracture interconnectivity.

FIELD INVESTIGATION

To conduct the field study, six 76 mm (N-sized) diameter boreholes were drilled in the vicinity of the site (Figure 1) using a diamond core and triple-tube wireline techniques. The boreholes were drilled to penetrate the entire thickness of the Lockport; a depth of approximately 55 m below ground surface. Five of the boreholes are inclined at angles ranging from 55° to 57° with respect to the ground surface, and one borehole (borehole 65) is vertical.

Once drilling was completed, hydraulic tests using the constant-head injection method (Novakowski, 1988) were performed on each borehole to obtain measurements of transmissivity over continuous 2 m depth intervals in each borehole. Minimum and maximum values of transmissivity ranging between 10^{-10} m²/s and 10^{-2} m²/s were determined using this procedure. After completion of the hydraulic testing, the boreholes were instrumented with a series of permanently-emplaced packer systems (Black et al., 1987). There are 5 - 9 isolated depth intervals in each borehole. Hydraulic head measurements in each isolated interval were obtained using a pressure transducer. Measurements of hydraulic head were obtained on a weekly basis over a two year period.

A total of 32 rock samples, collected from each of the geological units of the Lockport Formation, were submitted for chemical and mineralogical analyses. Samples were prepared by crushing the sample using a ceramic ball mill to a powder (<100 µm size fraction). Samples were analyzed for mineral content using X-Ray Diffraction (XRD) techniques. Concentrations of the major elements (SiO₂, TiO₂, Al₂O₃, Cr₂O₃, MnO, Fe₂O_{3 total}, MgO, CaO, Na₂O, K₂O and P₂O₅) and trace elements (Ba, Nb, Rb, Sr and Zr) were determined using wavelength dispersive x-ray fluorescence (XRF). Total concentrations of H₂O, CO₂ and S were determined using combustion followed by infrared spectrometry.

Groundwater samples were collected in November, 1997, from the permanently-emplaced packer systems. The samples were collected using a stainless steel sampling chamber (volume of 500 mL) connected to an electronic actuating device that draws in groundwater from the isolated zone outside the packer system. As the volume of water external to the packer system is relatively small, mixing and diffusional processes equilibrate the geochemical parameters in each isolated groundwater zone relatively quickly. Thus, the need to purge the borehole of standing water is eliminated (Black et al., 1987).

After drawing the sample to ground surface, electrical conductivity, Eh, and pH were measured in the field on unfiltered samples in enclosed containers. A combination electrode with an Ag/AgCl internal reference, calibrated against the buffers 4 and 7 were used to determine pH. Eh was measured using a combination platinum redox and Ag/AgCl reference electrode. Alkalinity was measured shortly after sample collection by titrating a known volume of filtered sample with 0.16N sulfuric acid using a HACH digital titrator. Groundwater samples collected for inorganic ions and dissolved organic carbon (DOC) analyses were filtered in the field using a 0.45 μm nylon filter. Samples submitted for cation analyses were preserved at the time of collection with ultrapure HCl.

Analyses for metals were performed in the laboratory using inductively coupled plasma spectroscopy (ICP-MS). Anions (Cl , SO_4 and SiO_2) were determined using ultraviolet photometry (COBAS). Concentrations of ammonia ($\text{NH}_3\text{-N}$) and nitrate ($\text{NO}_3\text{-N}$) were analyzed using a Bran+Luebbe TRAACS-800 continuous flow analyzer. Analyses for DOC were performed using ultraviolet digestion. Charge imbalances for the inorganic ions are less than 10% with the exception of 2 samples.

Samples were also collected for stable isotopes analyses (^{18}O and ^2H) in July and November of 1997. Analyses were performed using standard CO_2 /water and H_2 /water equilibration techniques.

$\delta^{18}\text{O}$ and $\delta^2\text{H}$ data were normalized to VSMOW/SLAP and are reported relative to VSMOW with reproducibility of ± 0.1 and ± 2.0 respectively. Samples were analyzed for ^3H by using direct scintillation methods obtaining a detection limit of 6TU, with a reproducibility of $\pm 8\text{TU}$. Eleven selected samples were re-analyzed for enriched ^3H analyses in order to refine the estimate of concentration of ^3H in the groundwater at a few locations. The enriched ^3H analyses has a reproducibility ranging between ± 0.6 to $\pm 1.3\text{ TU}$.

Saturation indices of various mineral phases were calculated using groundwater chemistry and the geochemical speciation program PHREEQC (Parkhurst, 1995). Thermodynamic data used for these calculations were provided in the PHREEQC database. The PHREEQC model calculations are considered reliable in sodium chloride dominated waters with higher ionic strength (Parkhurst, 1995).

RESULTS

Mineralogy

X-Ray Diffraction analyses (Table 1) indicate that the three principal minerals present in the units are dolomite (86-98 wt%), quartz (2-15 wt%) and gypsum (3-8 wt%). However, none of the samples from the Eramosa member are observed to contain any measurable gypsum. X-Ray Fluorescence analyses indicate that all samples have a Ca:Mg ratio between 1.03-1.09:1 (Table 1). Thus, most of the Ca in the samples is likely contained within the dolomite mineral structure. Any excess Ca concentrations will presumably exist as either calcite and/or gypsum. X-Ray Fluorescence analyses also indicates that both a small percentage of Fe and Al are present in the rock samples. Based on normative analyses of the rock chemistry and visual identification in the rock core, much of the Fe is likely incorporated in sulfide minerals (pyrite) whereas Al is likely to occur in clays.

Water Chemistry

Groundwater underlying the Smithville site (Table 2) is mainly reducing ($E_h < 0$) at depths greater than 20 to 30 m below ground surface (bgs). At shallow depths, conditions are more aerobic ($E_h > 0$ mV). Increased concentrations of HS^- in solution and subsequent decrease in Fe concentrations, suggest that redox conditions change from iron reducing to sulfate reducing with increasing depth. The pH of the groundwater is near neutral (6.8) to slightly alkaline (7.6). Temperature of the groundwater ranges from approximately 10 to 11 °C. Ion concentrations that increase with depth in solution are: Ca, Na, K, HS^- , Cl and SO_4 and those that decrease are: Mg and Fe. Alkalinity also decreases slightly with depth.

Hydraulic Properties

Constant head injection tests performed at continuous two meter depth intervals on each borehole indicate that transmissivity ranges between the testing limits of 10^{-10} m²/s and 10^{-2} m²/s. Highest transmissivities measured at the maximum level (10^{-2} m²/s) of the transmissivity test (3% of the total number of tests) are observed in boreholes 61, 63 and 65 at ~165, 155 and 170 meters above sea level (masl) respectively. Approximately 9% of the testing zones measured below the minimum testing limit (10^{-10} m²/s). Most of these zones are concentrated in the lower Vinemount and upper Rochester units. However, a few low transmissivity zones are observed at the top of the Goat Island (boreholes 60 and 62) adjacent to the Vinemount/Goat Island bedrock contact. The Eramosa, upper Vinemount and Gasport units are characterized by high transmissivities ranging from 10^{-5} to 10^{-2} m²/s, whereas many low transmissivity measurements (10^{-10} to 10^{-7} m²/s) are observed in the lower Vinemount unit and the Rochester Formation.

Hydraulic head measurements range from 181 masl to 192 masl. Highest head measurements are observed in the Eramosa member of boreholes 60, 62 and 63. In these boreholes, hydraulic head decreases sharply below the Eramosa member. Hydraulic head is observed to be almost uniform with depth in boreholes 53 and 65 with values ranging between 184 and 185 masl. In borehole 61 head is observed to be highest at an intermediate depth (at 160 masl), resulting in an artesian condition.

Environmental Isotopes

In general, stable isotopic composition of the groundwater ranges widely from -9 to -14 ‰ and -50 to -110 ‰ for $\delta^{18}\text{O}$ and $\delta^2\text{H}$ respectively. The isotopic composition of the groundwater is relatively enriched (-9 to -11 ‰ and -50 to -80 ‰ for $\delta^{18}\text{O}$ and $\delta^2\text{H}$ respectively) and changes little with depth in boreholes 60, 61, 62 and 63 whereas values become significantly depleted at ~165 masl and below in boreholes 53 and 65. Tritium values vary from below detection to values greater than 25TU.

DISCUSSION

Major ion analyses of the groundwater samples indicate that three chemically distinct zones are present in the flow system (Figure 3). At shallow depths (elevations > 170 masl) Mg and SO_4 are observed to be the highest concentration of ions in solution. At elevations between approximately 150 to 170 masl, Ca and SO_4 enriched waters dominate. At greatest depth (elevations <150 masl) in boreholes 53, 61, 63 and 65, the groundwater chemistry approaches brine conditions, characterized by high concentrations of Na and Cl.

The location of these chemical zones can be readily explained as a consequence of mineral dissolution and precipitation reactions. For instance, calculated saturation indices (Figure 4) indicate

that groundwater in most boreholes is undersaturated (SI ~ -0.5 to -1.0) with respect to gypsum at shallow depths (~ 20 to 30 m bgs or >165 masl). Below this, groundwater is observed to be close to equilibrium with gypsum (SI ~ 0) suggesting that the amount of Ca in the groundwater is controlled by chemical equilibration reactions with gypsum. At all depths groundwater tends to be undersaturated or near saturation with respect to both dolomite and calcite (Figure 4).

Mineralogical studies indicate that the geological members in the lower units contain a small percentage of gypsum whereas no gypsum was observed in the upper Eramosa member. Thus, the dissolution of dolomite and calcite alone will control the amount of Ca concentrations in the groundwater located in this upper unit. The presence of gypsum in the lower formation members indicates that undersaturated water (i.e. recharge water) has not extensively reached this horizon. The high Na concentrations and overall salinity observed in groundwater at greater depth (elevations of approximately 150 masl or less; Figure 3, Table 2) indicates high residence time and therefore sluggish groundwater velocity.

The measured hydraulic parameters (transmissivity and hydraulic head) in each borehole are compared to measured geochemical parameters (Figure 5). The boreholes are arranged based on location upgradient (boreholes 60, 62 and 63; Fig. 5a) of the PCB contaminated spill site, in an area of possible groundwater recharge versus those located either immediately adjacent to the site (boreholes 53, Figure 5b) or in possible areas of discharge along the river (boreholes 61 and 65; Figure 5b). Superimposed on these Figures are the distribution of the three chemically distinct groundwater zones discussed above.

Upgradient boreholes

Although the overburden is relatively thick in the vicinity of boreholes 60, 62 and 63, it was initially surmized that these boreholes are situated immediately downgradient from a potential zone of recharge. These boreholes are located approximately 1 km south of a swale which trends east-west. Due to a slight southward dip in the bedding planes, the thickness of the Eramosa member in these boreholes is less than that observed in the downgradient wells. The distribution of transmissivity follows the general observations (i.e. high transmissivity in the Eramosa, Goat Island and Gasport members). Lower transmissivities are observed in the middle to lower Vinemount member. An exception to this is borehole 62 which exhibits lower transmissivity throughout the base of the Eramosa, Vinemount and Goat Island members, with higher transmissivity evident only in the Gasport member.

The distribution of hydraulic head indicates a persistently downward gradient with increasing depth in all three boreholes. In each case, the transition between higher and lower hydraulic head occurs at the base of the Eramosa member or top of the Vinemount member, across a discrete zone of low transmissivity. In the case of borehole 60 and 63, the hydraulic head below the low transmissivity zone is uniform. The steady decrease in hydraulic head with depth observed in borehole 62 may indicate vertical fracture connection through these units within the immediate vicinity of this borehole.

Electrical conductivity is relatively uniform with depth in these boreholes, ranging from ~2000 μs to 4000 μs . Similarly, stable isotopic composition of the groundwater sampled is also uniform with depth, ranging from -9‰ to -11‰ and -60 ‰ and -80‰ for $\delta^{18}\text{O}$ and $\delta^2\text{H}$ respectively. Average $\delta^{18}\text{O}$ and $\delta^2\text{H}$ values in precipitation collected in Simco, Ontario, (located approximately 100 km to the east) during the period from 1975 to 1982, are approximately -10‰ and -70‰, respectively (IAEA/WMO). Thus, the groundwater is of recent origin. In addition, many of the sampled zones

contain measurable concentrations of ^3H indicating that groundwater in these zones is of post WWII age. In boreholes 60 and 62, ^3H concentrations are highest in the shallow depths (elevations >165 masl). However, high transmissivity zones in the lower Vinemount and Goat Island to upper Gasport also exhibit moderate to very high ^3H concentrations.

The fact that there is little change in electrical conductivity and in the stable isotopic signature with respect to depth suggests that in the upgradient boreholes, groundwater in both the upper Eramosa member and the in the lower members are of a common origin. The presence of ^3H at various depths (i.e. shallow and deep) further indicates that younger water is infiltrating the flow system. As the clay till overburden is thick and relatively impermeable overlying these boreholes, this suggests that recharge is localized to the swale and a bedrock ridge which lies immediately to the north of the site. Overburden thickness along this swale is minor and ranges from 1 to 2 m in thickness. The bedrock ridge immediately north of the swale has a topographic high of 10 - 15 m above the swale and consists of Eramosa member rocks. North of this ridge towards the escarpment, overburden thickness increases. Thus, the source of the water in the Eramosa is most likely the ridge and swale area.

Downgradient boreholes

In general, the lithology logs for boreholes 53, 61 and 65 show a diminished overburden thickness and an increase in the thickness of the Eramosa member in the downgradient direction (Figure 5b). The elevation of the top of the Rochester formation (the underlying aquitard) is 8 to 9 m below that of the upgradient boreholes.

The distribution of transmissivity in these boreholes is similar to that for the upgradient boreholes. Low transmissivity zones in the middle to lower Vinemount and high transmissivity zones in the Eramosa/Upper Vinemount, Goat Island and Gasport members are observed. The exception, is

borehole 65, which has more sparsely distributed zones of limited transmissivity (10^{-7} to 10^{-8} m²/s) in the Goat Island and Gasport members.

Contrary to the boreholes located upgradient, boreholes 53 and 65 have a relatively uniform distribution of hydraulic head with depth. The slightly lower hydraulic head observed at 175 masl (middle of the Eramosa member) in borehole 53 may be attributed to the ongoing pump-and-treat facility, located at the PCB spill site, that extends only a few meters into the upper bedrock. The hydraulic head distribution in borehole 61 is dissimilar to all other boreholes in that the highest hydraulic head is observed at 160 masl corresponding to the high transmissivity feature that straddles the Eramosa-Vinemount member contact. This zone is artesian, resulting in vertically upward and downward gradients emanating from this horizon.

The electrical conductivity in boreholes located downgradient generally increases with depth (Figure 5b) with the exception of borehole 61. The most profound change in electrical conductivity is observed in boreholes 53 and 65 where measured values range from 1500 μ S in the shallow zones to values greater than 20,000 μ S in the deepest zones. Electrical conductivity in borehole 65 is observed to steadily increase with depth, whereas in borehole 53 electrical conductivity mainly increases below the Eramosa - Vinemount contact located at 162 masl. In borehole 61 electrical conductivity increases only slightly from ~2000 to 5000 μ S.

In boreholes 53 and 65, $\delta^{18}\text{O}$ and $\delta^2\text{H}$ concentrations are relatively enriched in groundwater located in the Eramosa and Upper Vinemount members (>165 masl) with values ranging between -9 ‰ and -11 ‰ and -50 ‰ to -80 ‰ respectively. Below the Vinemount member, the isotopic signature becomes significantly more depleted with values ranging between -13 ‰ to -17 ‰ and -80 ‰ to -110 ‰ for $\delta^{18}\text{O}$ and $\delta^2\text{H}$, respectively. The change in isotopic signature occurs below the low transmissivity zone located in the Vinemount member. In both boreholes 53 and 65, ^3H (analyzed

by direct methods) is not observed in any of the sampled groundwater. However, enriched ^3H values obtained subsequently from borehole 53, indicate that the presence of ^3H (6.3TU \pm 0.8TU) at 175 masl, close to the contact between the Eramosa and Vinemount units. The isotopic composition of the groundwater in borehole 61 varies little with $\delta^{18}\text{O}$ and $\delta^2\text{H}$ ranging from -9‰ to -11‰ and -55‰ to -80‰ throughout the borehole depth. This signature is similar to that for the upgradient boreholes. As with the upgradient boreholes, substantial ^3H concentrations are also observed in borehole 61, particularly at the shallowest interval and the high transmissivity zone located in the middle of the Eramosa member. In borehole 65, a small amount of ^3H is observed at 150 masl. A second sample from this zone obtained 5 months later confirmed the presence of ^3H (3.8TU enriched \pm 1.3TU). However, this zone is of low transmissivity ($\sim 10^{-8} \text{ m}^2/\text{s}$) and it is likely that drill water was entrapped during installation of the permanent packer system. Dissolved chloride concentrations are elevated ($\sim 8000 \text{ mg/L}$) in this zone but not as elevated as that observed at the deepest levels in borehole 53 ($\sim 19,000 \text{ mg/L}$) which may suggest that drill water has not entirely equilibrated with groundwater.

The pronounced shift with depth in isotopic composition and electrical conductance observed in borehole 53 and 65 suggests that two distinct flow systems are present. As with the upgradient boreholes, the low transmissivity zone in the Vinemount member appears to be the dividing horizon between older water at depth and younger water present in the Eramosa member. The absence of ^3H concentrations observed in groundwater from the Eramosa member in borehole 65 suggests that, although this water is young, recharge in the immediate vicinity is unlikely.

Tritium, $\delta^{18}\text{O}$ and $\delta^2\text{H}$ concentrations in borehole 53 show the presence of recent water in the high transmissivity zone at the base of the Eramosa and the upper Vinemount. A value of 6.3 (\pm 0.8 TU) for enriched ^3H was obtained for this interval. The source for this water is likely through connection with the upgradient recharge area. Considering that groundwater velocities in the fractures

within the lower Eramosa range from 10 to 30 m/day (Radcliffe, 1997) and matrix porosities range from 5 to 15% (unpublished data), transport of the ^3H from the recharge area in a horizontal flow system can be simulated. Using the Tang et al (1981) solution, simulation of transport in a discrete fracture having an aperture of 500 μm , a velocity of 30 m/day and adjacent matrix porosity of 5% shows that ^3H concentrations as high as 15 TU are possible at borehole 53 when input conditions at borehole 60 (i.e. 30 TU) are employed. The low concentrations of ^3H present in the low transmissivity zone in the upper Goat Island is likely remnant drill water.

The results for borehole 61 are complicated by the presence of the artesian hydraulic head in the high transmissivity zone in the Lower Eramosa and Vinemount units. The water in this zone is observed to contain ^3H (15TU +/- 8) and shows a similar isotopic signature to water from the recharge area. The source of this water is uncertain. Hydraulic connection from the recharge zone may be present. However, the upper Eramosa is exposed on the river bottom at several locations both upstream and downstream from borehole 61. Thus, it is more likely that the source of this water is through connection with river water in the stream direction of river flow.

Groundwater in the stratigraphic intervals and below the artesian zone show stable isotopic signatures similar to that in the artesian zone. Although these waters do not contain measurable ^3H , it is likely that they originate from the artesian zone, through vertical connections, or are recharged at locations further up the river valley.

CONCEPTUAL MODEL AND CONCLUSIONS

Since fracture networks are, in general, complex with the nature of fracture interconnection being uncertain, interpretation of groundwater flow from borehole to borehole using hydraulic parameters is difficult. The previous discussion supplements the hydrological data with geochemical

data to provide evidence for hydraulic interconnection on a large scale. The conceptual model (Figure 6) represents a two dimensional cross-section, using three selected boreholes located in the direction of groundwater flow (northwest to southeast).

Hydraulic head and measurements of transmissivity can provide only a general idea of groundwater flow in the immediate vicinity of a particular borehole. For example, the uniform distribution of hydraulic head in boreholes 53 and 65 coupled with large variations observed in transmissivity measurements may indicate that groundwater flow is primarily horizontal in the vicinity of these boreholes, with little interaction between the individual fracture planes. Alternatively, the uniformity of the hydraulic head distribution could imply that the horizontal fracture planes are extremely well connected such that no vertical gradient could exist. However, the chemistry and isotopic composition of the groundwater in these boreholes shows the water above the Vinemount to be markedly different than that below, suggesting that little interaction between the water in these two horizons has occurred. We can also infer from the uniformity in hydraulic head that there are no local groundwater sources (recharge zones) or drains (discharge zones) nearby.

Conversely, in the upgradient boreholes and borehole 61, transmissivity measurements are equally varied, yet distribution of hydraulic head with depth is not uniform. The change in hydraulic gradient with depth may suggest a large amount of vertical groundwater interaction or this could be just another manifestation of horizontal flow. Evidence for horizontal flow is provided by the geochemical results which show that the sharp change in hydraulic head distribution occurring at 175 masl in the upgradient boreholes (60, 62 and 63) divides two separate flow systems. The presence of ^3H at depths below the low transmissive zone (e.g. borehole 60) suggests that even though there is limited vertical hydraulic connection, there is enough to allow for the penetration of some freshwater across the low transmissive barrier. Thus, in both the upgradient and downgradient vicinities

groundwater flow is predominantly horizontal. Flow is likely controlled by large bedding plane fractures that have been observed in the Lockport formation (Tesmer, 1981, Novakowski and Lapcevic, 1988, Yager and Kappel, 1998). The presence of bedding-plane partings is common in sedimentary rock sequences and are usually caused by stress changes. Enlarged bedding plane partings have been found to control groundwater flow in the Lockport formation at Niagara Falls Ontario, and in the Newark Basin, New Jersey (Novakowski and Lapcevic, 1988, Michalski and Britton, 1997).

The uniformity of the stable isotope composition with depth in the upgradient holes (60, 62 and 63) and the overall similarity to that of recent precipitation values, suggests that groundwater recharge is occurring upgradient of these boreholes. Groundwater recharge for the area likely occurs through the Eramosa unit and is localized to the swale and ridge located immediately north of the upgradient boreholes, where overburden thickness is minimal.

In all boreholes, a zone of low transmissivity is located in the middle to lower Vinemount member. This zone of low transmissivity varies in thickness yet appears ubiquitously. It is this horizon of low transmissivity that separates groundwater flow into the upper and lower flow regimes in the region. The upper flow regime is present in the Eramosa member, the lower flow regime is present mainly in the Gasport and Goat Island members (Figure 6).

Inorganic ion concentrations of groundwater and subsequent geochemical speciation modeling suggests that these regimes are physically and chemically related to the geological bedrock. Shallow groundwater is found to be dominated by high Mg concentrations due to equilibrium reactions with dolomite which control the amount of Ca and Mg in solution. However, in the lower flow regime, groundwater is dominated by high Ca and SO_4 concentrations due to the higher amount of gypsum minerals present in the rocks.

Transmissivity measurements in the lower flow regime are observed to be just as high as that in the upper flow regime. Thus, calculations based on equivalent aperture width would suggest that groundwater velocity in both flow regimes should be similar. However, the high electrical conductivity observed in the downgradient boreholes 53 and 65 at depth indicates that groundwater residence time in this zone is much greater than in the upper zone. Also, the observed depletion in stable oxygen and hydrogen isotopes at depth in these boreholes suggest that there is relatively less dilution from younger recharge water. As recharge is observed to occur in both regimes in the upgradient boreholes, it is therefore implied, through geochemical observation, that groundwater velocity in the lower flow regime is considerably slower than that in the upper flow regime.

Groundwater discharge from the flow system is less well defined. At borehole 65 located upstream of the town of Smithville along the banks of 20 mile creek, groundwater in both the upper and lower flow systems appears to completely underflow the river. However, at borehole 61 located downstream from the town center, groundwater appears to interact with the river water, at least within the upper flow system. In borehole 61, a high transmissivity zone in the Goat Island/Gasport exhibits the lowest hydraulic head at depth of any of the boreholes. This indicates significant underflow of the lower flow system although most of the water appears to be entrained in the direction of river flow.

ACKNOWLEDGEMENTS

Gratitude is extended to Kelly Millar, Susan Brown and Andrea Brown for their assistance in the laboratory and the field. Also appreciated are editing suggestions from Jos Beckers, and suggestions from Amy Sheldon in the interpretation of the tritium analyses. Funding for this research was provided by the Smithville Phase IV project.

REFERENCES

- Black, W.H., Smith, H.R., and Patton, F.D., 1987. Multiple-level groundwater monitoring with the MP system, In: Proceedings NWWA-AGU Conf. Surface and Borehole Geophysical Methods and Groundwater Instrumentation, NWWA, Dublin, Ohio.
- Foster, S.S.D., 1975. The Chalk groundwater tritium anomaly – A possible explanation. *J. Hydrol.*, 25: 159-165.
- Faure, G., 1986. *Principals of Isotope Geology*. John Wiley and Sons. New York, N.Y., 589 pp.
- Golder Associates Ltd., 1995. Hydrogeologic data compilation and assessment,, CWML Site. Smithville, Ontario. Golder Associates Ltd. Report No. 941-9033.
- Hisscock, K.M., Dennis, P.F., Saynor, P.R. and Thomas M.O., 1996. Hydrochemical and stable isotope evidence for the extent and nature of the effective Chalk aquifer of north Norfolk, UK. *J. Hydrol.*, 180: 79-107.
- IAEA/WMO (1998). Global Network for Isotopes in Precipitation. The GNIP database. Release 2 May, 1998. Simco, Ontario. www.iaea.org
- Maslia, M.L. and Johnston, R. H., 1984. Use of a digital model to evaluate hydrogeologic controls on groundwater flow in a fractured rock aquifer at Niagara Falls, New York, U.S.A. *J. of Hydrol.*, 75: 167-194.
- Michalski, A. and Britton, R., 1997. The role of bedding fractures in the hydrogeology of sedimentary bedrock - Evidence from the Newark Basin, New Jersey. *Ground Water*, 35(2): 318 -327.
- Novakowski, K.S. 1988. Comparison of fracture aperture widths determined from hydraulic measurements and tracer experiments. In: Fluid Flow, Heat Transfer and Mass Transport in Fractured Rocks, Proceedings of the 4th Canadian/American Conference on Hydrogeology. B. Hitchon and S. Bachu (Editors). June 21- 24, 1988, Banff, Alberta. National Water Well Association, Dublin, Ohio. pp. 68-80.
- Novakowski, K.S. and P.A. Lapcevic. 1988. Regional hydrogeology of the Silurian and Ordovician sedimentary rock underlying Niagara Falls, Ontario, Canada. *J. Hydrol.*, 104:211-236.
- Parkhurst, D.L., 1995. User's guide to PHREEQC - A computer program for speciation, reaction-path, advective-transport and inverse geochemical calculations. U.S. Geological Survey, Water-Resources Investigations Report 95-4227, 143 pp.
- Radcliffe, A., 1997. Determination of Groundwater Velocities in Discrete Fractures using Point Dilution Methods. B.Sc. thesis, University of Waterloo, 26 p.

Riechart, T. M., 1992. Influence of vertical fractures in horizontally stratified rocks. Unpublished M.Sc. Thesis. University of Waterloo, Ontario., 92p.

Smellie, J.A.T., Laaksoharju, M., and Wikberg, P., 1995. Aspo, SE Sweden: a natural groundwater flow model derived from hydrogeochemical observations. J. Hydrol., 172: 127-146.

Tang, D.H., Frind, E. d. and Sudicky, E.A., 1981. Contaminant transport in fractured porous media. Analytical solution for a single fracture. Wat. Res. Res., 17(3):555-564.

Tesmer, I.H., 1981. *Colossal Cataract, The Geological History of Niagara Falls*. State University of New York Press, Albany, N.Y., 219 pp.

Yager, R.M., Bilotta, S.E., Mann, C.L. and Madsen, E.L., 1997. Metabolic adaptation and in situ attenuation of chlorinated ethenes by naturally occurring microorganisms in a fractured dolomite aquifer near Niagara Falls, New York. Environ. Sci. Technol., 31: 3138-3147.

Yager, R.M. and Kappel, W.M., 1998. Infiltration and hydraulic connections from the Niagara River to a fractured-dolomite aquifer in Niagara Falls, New York. Journal of Hydrology, 206:84-97.

FIGURE CAPTIONS

Figure 1: Topographical map of the Smithville field site and borehole locations.

Figure 2: General stratigraphy of the Lockport Formation.

Figure 3: Piper diagram for groundwater chemistry of samples collected from Westbay packer installed boreholes.

Figure 4: Calculated saturation indices using PHREEQC for dolomite, gypsum and calcite using chemistry from groundwater samples collected at selected borehole depths.

Figure 5: Composite diagram of measured parameters in a) boreholes 60, 62 and 63 located upgradient from the PCB spill site and b) boreholes 53, 61 and 65 located downgradient from the PCB spill site. e; represents enriched ^3H values.

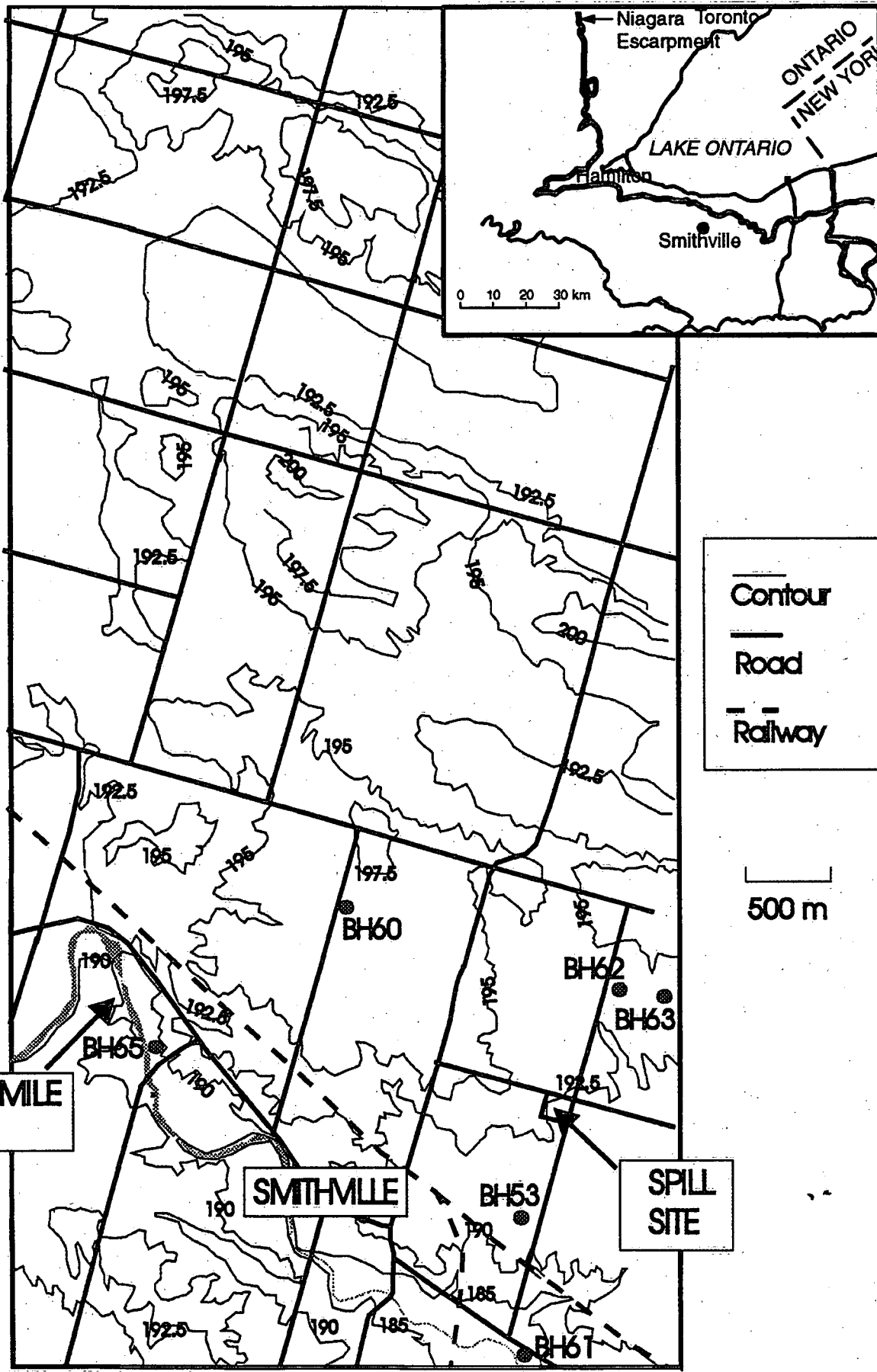
Figure 6: Conceptual model of two dimensional flow at the Smithville site in the general direction of groundwater flow.

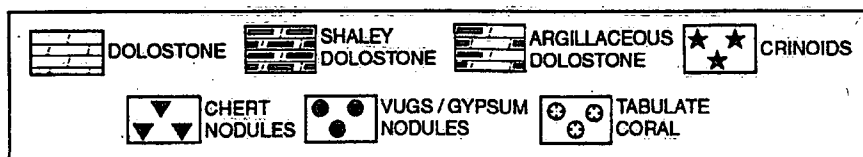
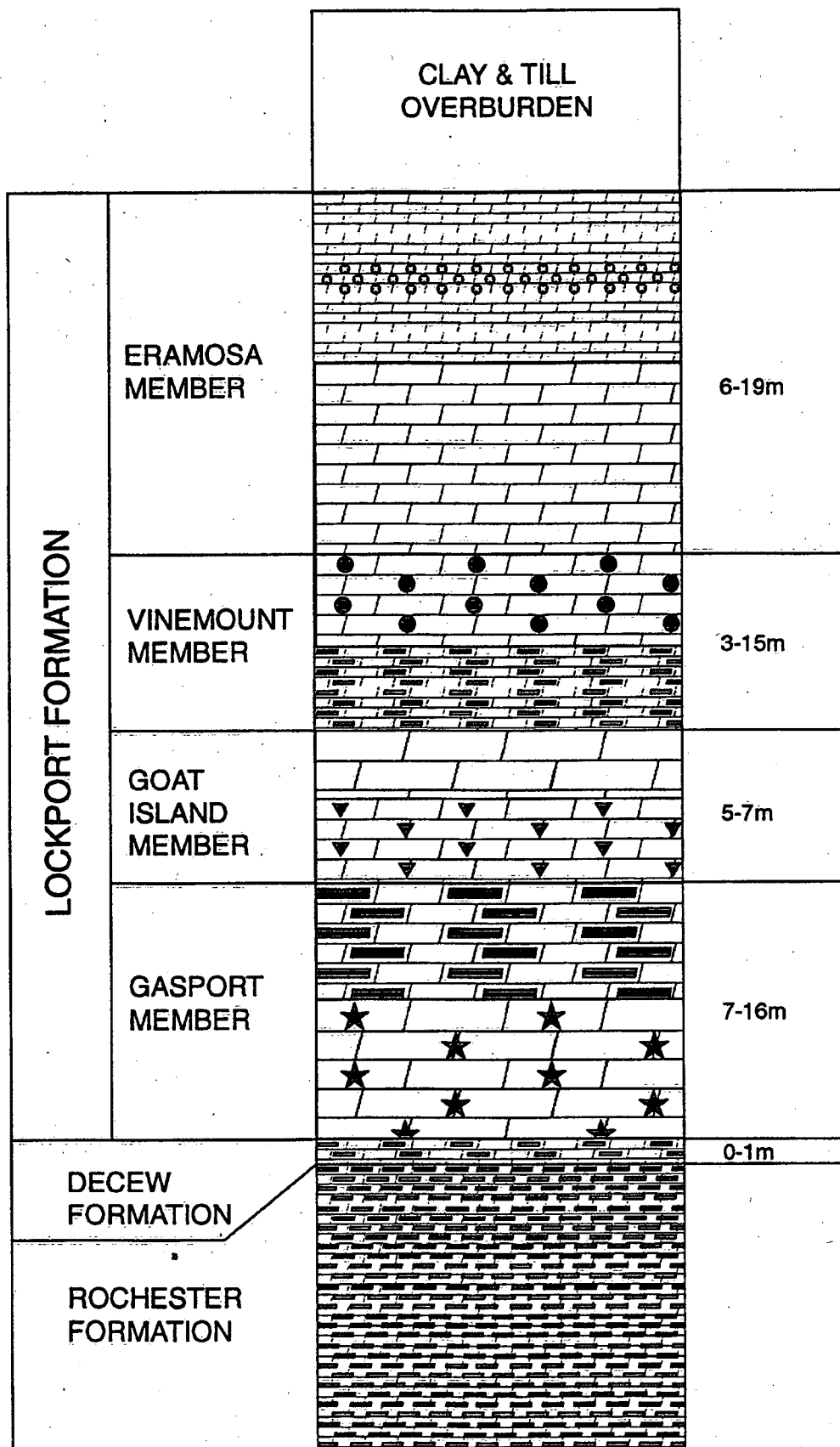
Table 1: XRF and XRD analyses of rock samples collected from various geological units at the Smithville site.

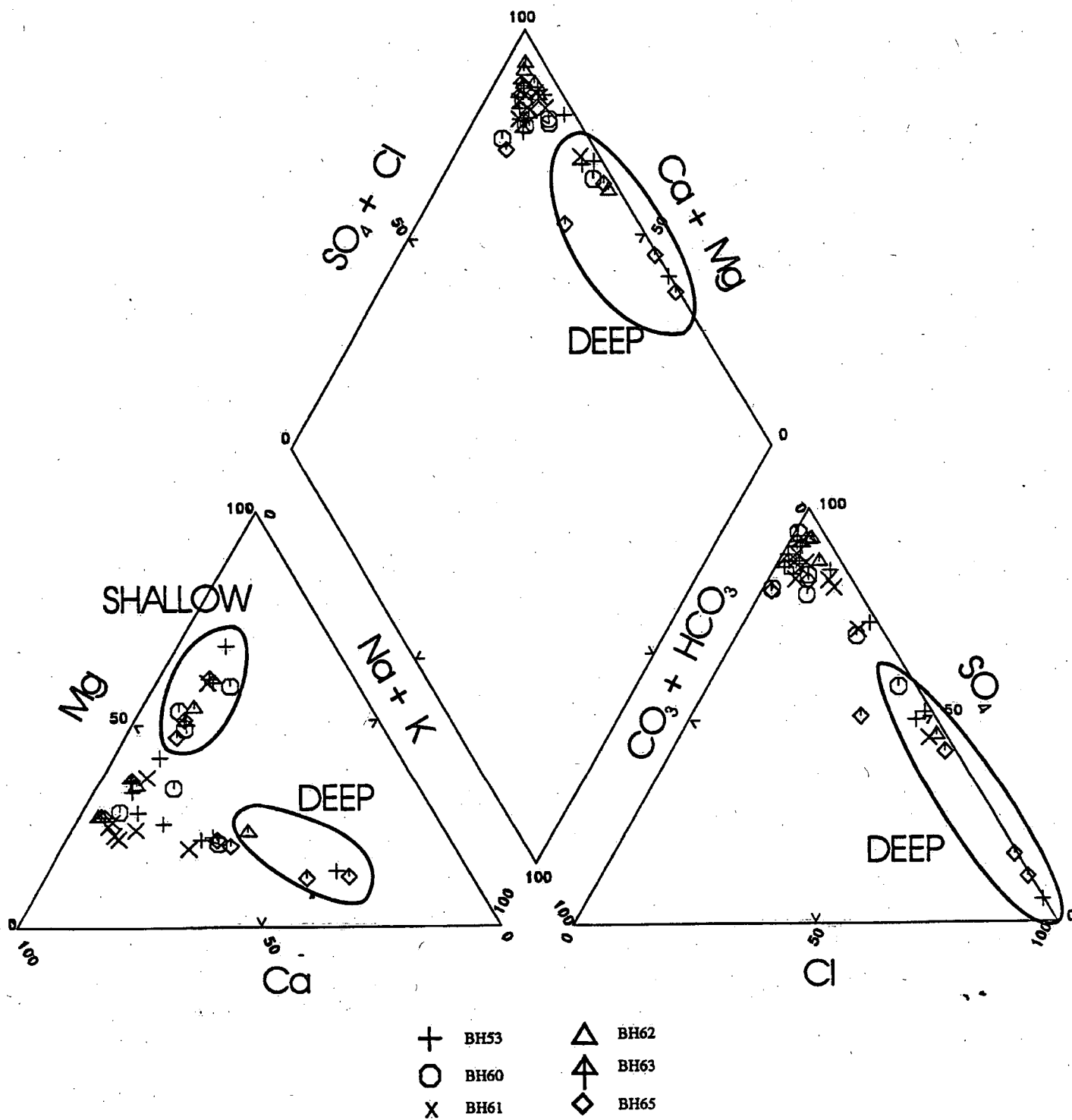
| Formation /Member | Elevation (masl) | Si (mmol) | Ti (mmol) | Al (mmol) | Fe(total) (mmol) | Mn (mmol) | Mg (mmol) | Ca (mmol) | K (mmol) | H ₂ O (mmol) | C (mmol) | P (mmol) | S (mmol) | Dolomite (%) | Quartz (%) | Gypsum (%) | Calcite (%) |
|-------------------|------------------|-----------|-----------|-----------|------------------|-----------|-----------|-----------|----------|-------------------------|----------|----------|----------|--------------|------------|------------|-------------|
| Eramosa | 183.3 | 16.6 | 0.13 | 5.88 | 1.25 | 0.42 | 512 | 538 | 0.64 | 33.3 | 1059 | 0.14 | 1.25 | 97.3 | 2.7 | | 3.8 |
| Eramosa | 179.9 | 5.0 | 0.00 | 1.96 | 0.00 | 0.70 | 515 | 546 | 0.21 | 27.8 | 1059 | 0.28 | 1.25 | 93.7 | 2.5 | | |
| Eramosa | 176.1 | 18.3 | 0.13 | 5.88 | 2.50 | 0.85 | 511 | 535 | 0.85 | 33.3 | 1061 | 0.70 | 2.81 | 97.1 | 2.9 | | |
| Eramosa | 171.6 | 3.3 | 0.13 | 1.96 | 2.50 | 1.41 | 522 | 540 | 0.00 | 11.1 | 1079 | 0.14 | 0.62 | 87.0 | 0.0 | | |
| Eramosa | 168.5 | 3.3 | 0.00 | 1.96 | 3.76 | 2.11 | 521 | 539 | 0.00 | 16.7 | 1079 | 0.14 | 0.62 | 97.6 | 2.4 | | |
| Vinemount 2 | 173.5 | 110 | 1.38 | 49.0 | 12.5 | 0.99 | 458 | 481 | 13.4 | 66.6 | 961 | 0.85 | 16.2 | 94.0 | 6.0 | | |
| Vinemount 2 | 165.6 | 86.5 | 1.13 | 39.2 | 10.0 | 0.85 | 474 | 495 | 8.07 | 66.6 | 979 | 0.70 | 13.4 | 96.9 | 3.1 | | |
| Vinemount 2 | 139.7 | 61.6 | 0.38 | 13.7 | 5.01 | 1.13 | 489 | 521 | 2.55 | 44.4 | 998 | 0.56 | 9.98 | 91.1 | 5.5 | 3.4 | |
| Vinemount 1 | 173.9 | 102 | 0.50 | 21.6 | 10.0 | 1.27 | 467 | 504 | 5.52 | 38.9 | 973 | 0.42 | 13.7 | 91.6 | 8.4 | | |
| Vinemount 1 | 172.9 | 35.0 | 0.50 | 11.8 | 5.01 | 0.85 | 496 | 529 | 2.12 | 36.9 | 1032 | 0.42 | 7.17 | 89.3 | 3.0 | 7.7 | |
| Vinemount 1 | 171.6 | 138 | 0.88 | 15.7 | 11.3 | 1.97 | 459 | 493 | 4.67 | 44.4 | 948 | 0.42 | 21.2 | 87.6 | 8.7 | 3.6 | |
| Vinemount 1 | 161.6 | 74.9 | 0.63 | 17.7 | 5.01 | 1.13 | 482 | 514 | 3.82 | 50.0 | 995 | 0.28 | 9.05 | 89.8 | 2.8 | 7.4 | |
| Vinemount 1 | 159.5 | 84.9 | 0.63 | 17.7 | 5.01 | 0.99 | 480 | 511 | 4.25 | 38.9 | 995 | 0.28 | 7.17 | 92.4 | 7.6 | | |
| Vinemount 1 | 156.0 | 33.3 | 0.25 | 7.85 | 2.50 | 0.85 | 506 | 531 | 1.06 | 27.8 | 1043 | 0.14 | 3.12 | 96.3 | 3.7 | | |
| Goat Island | 169.7 | 107 | 0.88 | 25.5 | 7.51 | 0.99 | 473 | 498 | 6.37 | 38.9 | 975 | 0.28 | 8.42 | 93.7 | 6.3 | | |
| Goat Island | 168.2 | 38.3 | 0.38 | 11.8 | 6.26 | 1.27 | 501 | 529 | 2.12 | 27.8 | 1036 | 0.42 | 5.61 | 96.7 | 3.3 | | |
| Goat Island | 168.1 | 13.3 | 0.13 | 3.92 | 3.76 | 1.13 | 513 | 537 | 0.21 | 22.2 | 1066 | 0.28 | 1.56 | 91.7 | 2.0 | 6.3 | |
| Goat Island | 157.6 | 15.0 | 0.00 | 3.92 | 3.76 | 1.55 | 516 | 536 | 0.21 | 16.7 | 1068 | 0.28 | 0.62 | 96.4 | 3.6 | | |
| Goat Island | 154.4 | 13.3 | 0.00 | 1.96 | 3.76 | 1.13 | 516 | 536 | 0.21 | 22.2 | 1068 | 0.28 | 0.94 | 96.7 | 3.3 | | |
| Goat Island | 150.8 | 25.0 | 0.13 | 7.85 | 5.01 | 0.85 | 508 | 532 | 1.06 | 33.3 | 1045 | 0.56 | 5.61 | 96.6 | 3.4 | | |
| Gasport | 163.9 | 13.3 | 0.13 | 5.88 | 5.01 | 1.27 | 494 | 541 | 0.42 | 61.1 | 1011 | 0.14 | 25.9 | 93.2 | 2.1 | 4.6 | |
| Gasport | 163.1 | 53.3 | 0.13 | 5.88 | 3.76 | 1.13 | 498 | 524 | 0.64 | 27.8 | 1038 | 0.28 | 1.87 | 90.0 | 3.0 | | |
| Gasport | 160.3 | 24.5 | 0.88 | 29.4 | 10.0 | 1.55 | 422 | 447 | 7.43 | 38.9 | 875 | 0.42 | 9.67 | 84.5 | 15.5 | | |
| Gasport | 155.7 | 43.3 | 0.63 | 17.7 | 6.26 | 0.99 | 496 | 521 | 2.55 | 33.3 | 1009 | 0.42 | 3.12 | 97.8 | 2.4 | | |
| Gasport | 153.8 | 94.9 | 1.00 | 43.2 | 6.26 | 0.56 | 474 | 493 | 10.6 | 50.0 | 961 | 0.70 | 4.37 | 96.3 | 3.7 | | |
| Gasport | 151.5 | 117 | 0.88 | 31.4 | 5.01 | 0.99 | 468 | 489 | 8.49 | 44.4 | 966 | 0.42 | 2.81 | 92.1 | 7.9 | | |
| Gasport | 145.4 | 28.3 | 0.25 | 7.85 | 5.01 | 1.41 | 499 | 537 | 0.85 | 50.0 | 1018 | 0.42 | 15.0 | 91.2 | 2.3 | 6.5 | |
| Rochester | 154.6 | 115 | 0.50 | 15.7 | 10.0 | 1.69 | 469 | 499 | 2.97 | 33.3 | 970 | 0.56 | 8.42 | 92.1 | 7.9 | | |
| Rochester | 153.1 | 81.6 | 0.50 | 15.7 | 7.51 | 1.27 | 481 | 512 | 2.97 | 33.3 | 993 | 0.56 | 7.80 | 93.0 | 7.0 | | |
| Rochester | 147.1 | 251 | 2.38 | 90.2 | 17.5 | 0.85 | 398 | 413 | 28.5 | 77.7 | 809 | 0.56 | 20.90 | 87.5 | 12.5 | | |
| Rochester | 141.3 | 253 | 2.75 | 96.1 | 18.8 | 0.85 | 393 | 409 | 30.4 | 88.8 | 798 | 0.56 | 21.52 | 73.3 | 6.2 | | |

Table 2: Geochemical analyses of groundwater samples collected from boreholes at selected depths.

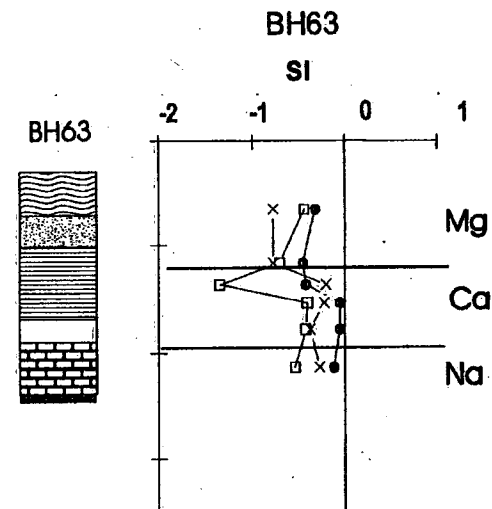
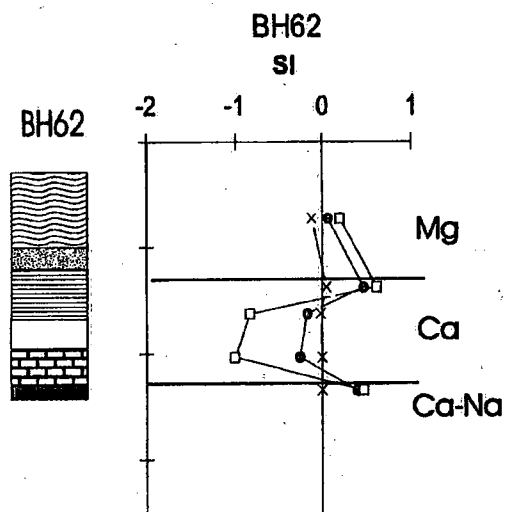
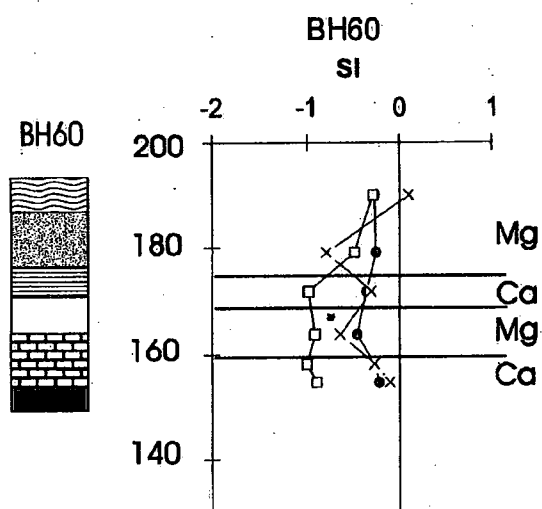
| Borehole | Bottom zone (masl) | Top zone (masl) | pH | Eh (mV) | Alkalinity (mg/L CaCO ₃) | Ca (mg/L) | Mg (mg/L) | Na (mg/L) | K (mg/L) | Fe (mg/L) | SO ₄ (mg/L) | Cl (mg/L) | HS (mg/L) | SiO ₂ (mg/L) |
|----------|-----------------------|--------------------|-----|------------|---|--------------|--------------|--------------|-------------|--------------|---------------------------|--------------|--------------|----------------------------|
| 53 | 176.4 | 191.8 | 6.9 | 320 | 300 | 268 | 477 | 127 | 7.00 | 1.67 | 2810 | 64.2 | 0.00 | 16.3 |
| | 173.9 | 175.7 | 7.2 | 259 | 180 | 214 | 72 | 32.2 | 2.40 | 0.35 | 628 | 6.70 | 0.02 | 12.7 |
| | 167.6 | 173.2 | 7.2 | 195 | 125 | 132 | 97 | 41.0 | 2.60 | 0.46 | 519 | 16.2 | 0.00 | 13.3 |
| | 162.6 | 166.9 | 7.2 | 29 | 257 | 250 | 125 | 53 | 4.20 | 0.16 | 847 | 34.7 | 0.79 | 12.9 |
| | 157.6 | 161.9 | 7.3 | -30 | 138 | 662 | 178 | 451 | 25.3 | 0.13 | 1840 | 1290 | 3.42 | 7.46 |
| | 151.3 | 156.8 | 6.6 | -100 | 209 | 558 | 154 | 116 | 12.5 | 0.09 | 2105 | 216 | 4.48 | 7.06 |
| | 146.3 | 150.5 | 7.0 | -80 | 127 | 575 | 153 | 206 | 10.5 | 0.07 | 1920 | 514 | 5.86 | 8.32 |
| | 142.5 | 145.5 | 6.9 | -94 | 292 | 663 | 164 | 407 | 5.91 | 0.05 | 1495 | 1061 | 5.56 | 8.50 |
| | 139.0 | 141.7 | 6.3 | -103 | 180 | 2900 | 847 | 7000 | 137 | 0.05 | 1457 | 18917 | 5.68 | 26.4 |
| 60 | 183.1 | 197.0 | 6.9 | 98 | 400 | 400 | 520 | 260 | 5.70 | 10.60 | 2943 | 19.4 | 0.09 | 15.9 |
| | 175.7 | 182.4 | 7.2 | 155 | 291 | 140 | 110 | 31.3 | 2.20 | 0.01 | 616 | 11.4 | 0.04 | 13.0 |
| | 168.2 | 174.9 | 7.0 | -78 | 234 | 338 | 136 | 119 | 8.10 | 0.05 | 1185 | 315 | 5.81 | 10.2 |
| | 159.9 | 167.4 | 7.1 | -53 | 248 | 173 | 122 | 51.9 | 5.20 | 0.09 | 794 | 72.5 | 2.31 | 12.7 |
| | 156.6 | 159.2 | 7.0 | 93 | 268 | 342 | 90 | 45.1 | 5.40 | 1.13 | 1172 | 80.6 | 0.27 | 13.7 |
| | 153.0 | 155.8 | 7.0 | -62 | 255 | 507 | 127 | 370 | 19.3 | 0.06 | 1679 | 864 | 3.64 | 11.7 |
| 61 | 175.0 | 182.2 | 7.0 | -9 | 300 | 248 | 285 | 92.9 | 6.20 | 1.00 | 1430 | 34.8 | 0.29 | 14.9 |
| | 170.1 | 174.3 | 6.9 | -13 | 310 | 387 | 83 | 44.4 | 4.40 | 0.09 | 1265 | 58.0 | 3.35 | 12.5 |
| | 165.2 | 169.4 | 7.0 | -25 | 218 | 447 | 103 | 56 | 3.80 | 0.06 | 1120 | 56.5 | 3.07 | 12.3 |
| | 155.4 | 164.5 | 7.0 | -22 | 237 | 278 | 112 | 51.7 | 4.00 | 0.03 | 763 | 38.7 | 1.77 | 12.8 |
| | 151.7 | 154.6 | 6.9 | -65 | 204 | 465 | 91 | 70.8 | 6.50 | 0.06 | 1443 | 163 | 6.13 | 9.83 |
| | 145.5 | 150.9 | 6.8 | -63 | 232 | 538 | 121 | 127 | 6.90 | 0.07 | 1450 | 373 | 5.81 | 9.38 |
| | 141.9 | 144.8 | 7.0 | -28 | 230 | 562 | 107 | 100 | 6.70 | 0.09 | 1678 | 224 | 2.13 | 11.0 |
| | 138.4 | 141.1 | 7.1 | 10 | 231 | 600 | 125 | 324 | 13.7 | 2.08 | 1196 | 1025 | 0.13 | 9.42 |
| 62 | 175.0 | 195.4 | 7.4 | 118 | 285 | 392 | 341 | 129 | 5.00 | 9.69 | 2270 | 164 | 0.00 | 12.7 |
| | 171.3 | 173.4 | 7.7 | 47 | 245 | 551 | 197 | 85.0 | 10.2 | 5.20 | 2350 | 75.2 | 0.00 | 7.46 |
| | 163.9 | 170.6 | 7.1 | -92 | 206 | 537 | 127 | 36.0 | 10.2 | 0.05 | 1745 | 44.5 | 5.35 | 7.90 |
| | 155.2 | 163.1 | 7.1 | -95 | 176 | 520 | 120 | 30.4 | 7.70 | 0.06 | 1933 | 67.5 | 5.11 | 7.41 |
| | 151.4 | 154.5 | 7.6 | 28 | 204 | 710 | 238 | 704 | 25.5 | 4.52 | 1903 | 1654 | - | 7.42 |
| 63 | 179.6 | 194.3 | 7.3 | 162 | 214 | 149 | 177 | 65 | 2.80 | 1.83 | 672 | 11.1 | 0.01 | 14.5 |
| | 174.7 | 178.6 | 7.3 | 153 | 204 | 139 | 167 | 53.9 | 2.60 | 1.7 | 742 | 14.3 | 0.00 | 13.9 |
| | 171.4 | 173.7 | 6.9 | 103 | 224 | 376 | 88.7 | 32.4 | 4.50 | 1.77 | 1310 | 17.4 | 0.02 | 13.0 |
| | 167.7 | 170.4 | 7.3 | 92 | 231 | 352 | 129 | 43.1 | 4.40 | 5.95 | 1334 | 31.1 | 0.12 | 11.8 |
| | 161.6 | 166.7 | 7.3 | 101 | 216 | 323 | 117 | 39.1 | 4.50 | 5.43 | 923 | 37.4 | 0.10 | 11.9 |
| | 153.4 | 160.6 | 7.3 | 94 | 193 | 359 | 134 | 43.5 | 4.30 | 3.38 | 1176 | 31.0 | 0.22 | 11.1 |
| | 145.6 | 148.0 | 6.8 | -105 | 144 | 1650 | 340 | 2900 | 57.1 | 0.051 | 1280 | 7700 | - | 6.65 |
| 65 | 175.2 | 180.5 | 7.1 | 14 | 204 | 114 | 86 | 32.0 | 2.60 | 0.232 | 418 | 8.2 | 0.76 | 15.6 |
| | 164.7 | 174.0 | 7.0 | 179 | 229 | 268 | 170 | 72.0 | 5.40 | 2.98 | 912 | 70.0 | 0.49 | 12.9 |
| | 159.2 | 163.5 | 6.9 | -115 | 177 | 753 | 191 | 624 | 32.0 | 0.053 | 1390 | 1410 | 4.93 | 6.84 |
| | 153.7 | 158.0 | 6.9 | -80 | - | 1010 | 273 | 1500 | 31.6 | 0.045 | 1440 | 1300 | 4.42 | 6.24 |
| | 149.2 | 152.5 | 6.7 | -105 | 145 | 798 | 225 | 2190 | 42.6 | 0.049 | 1450 | 5490 | 3.56 | 6.27 |
| | 145.6 | 148.0 | 6.8 | -105 | 144 | 1650 | 340 | 2900 | 57.1 | 0.051 | 1280 | 7700 | - | 6.65 |



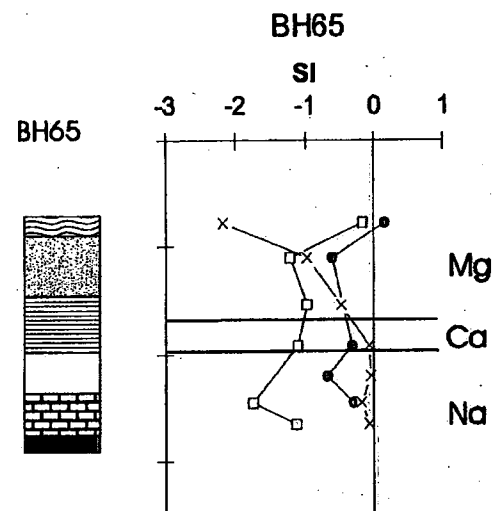
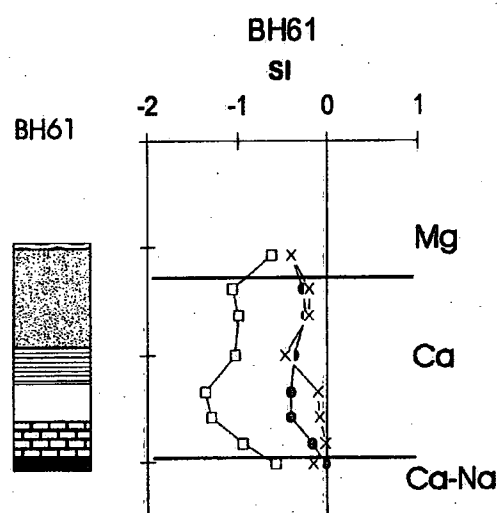
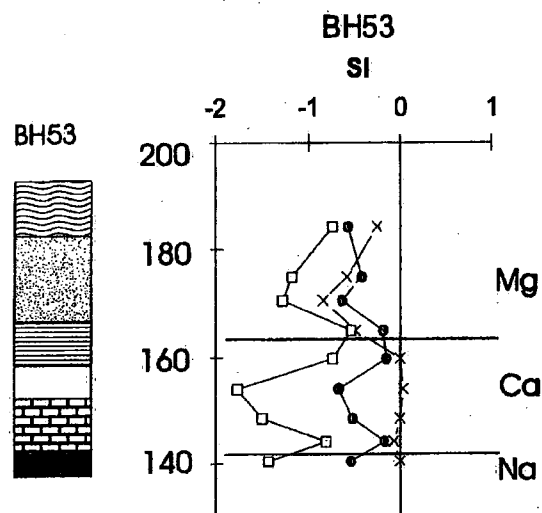




masl



masl



— Separation of differing groundwater chemical composition
 ○—○ Calcite saturation indices
 x—x Gypsum saturation indices
 □—□ Dolomite saturation indices

Overburden

Vinemount

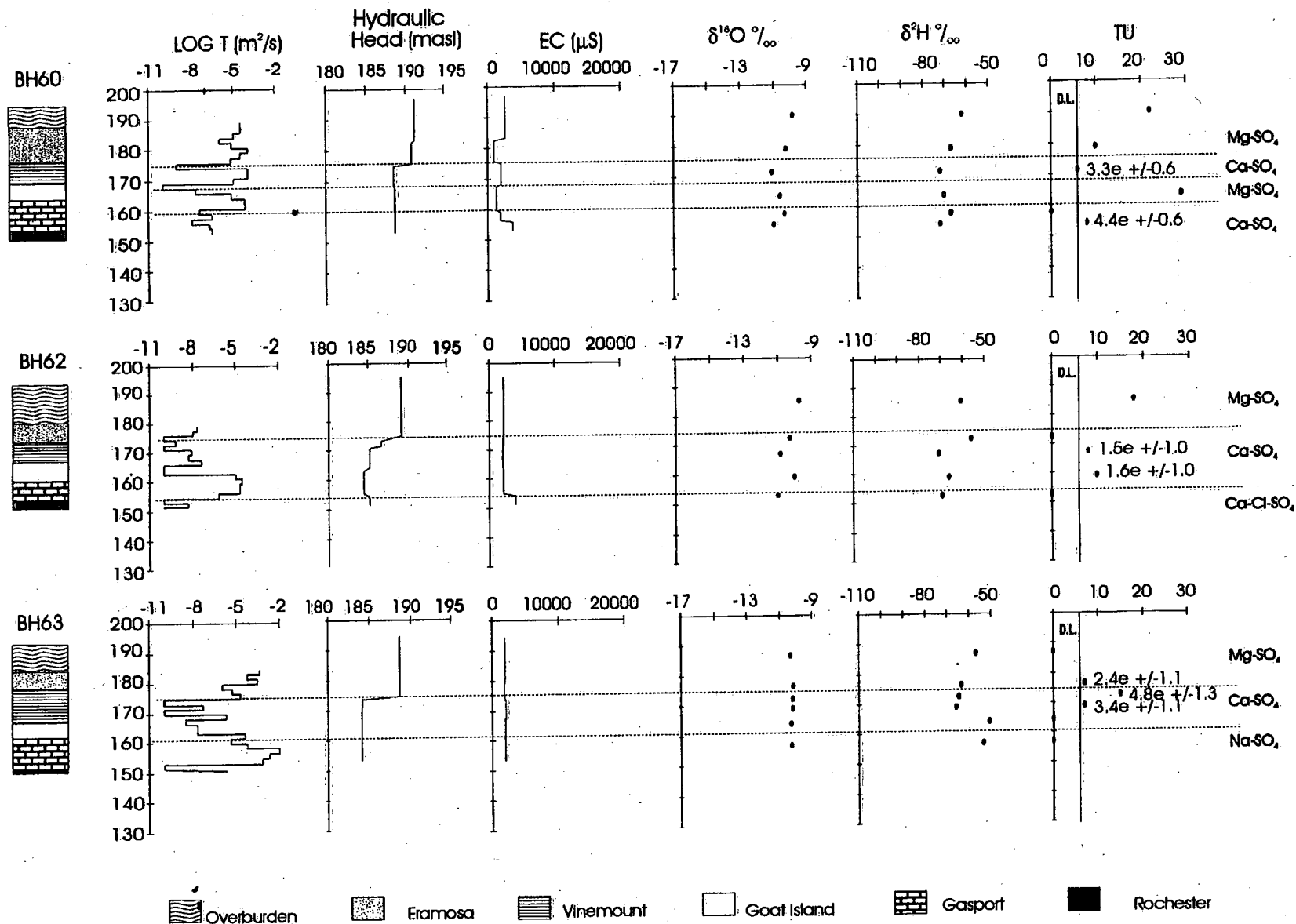
Gasport

Eramosa

Goat Island

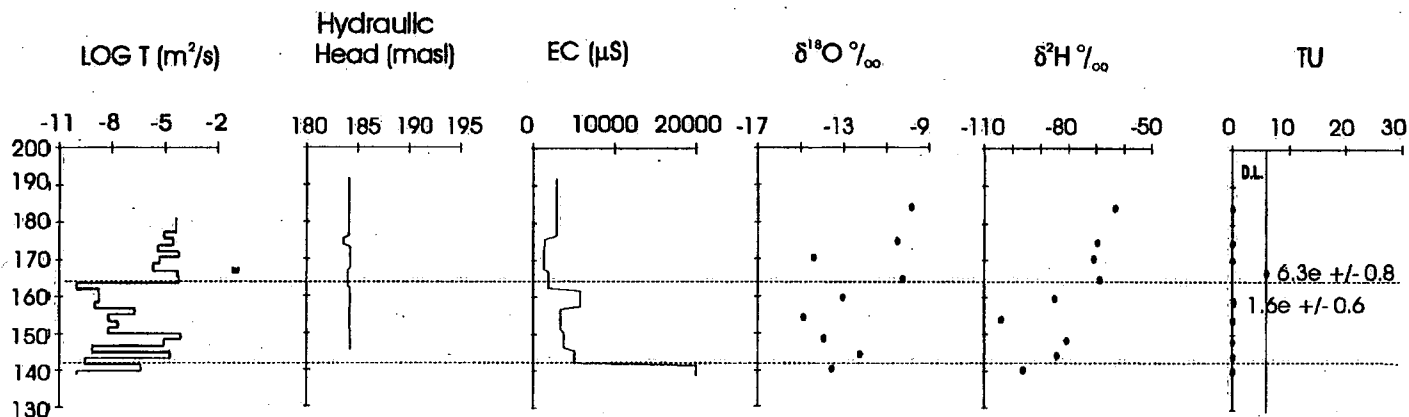
Rochester

MASL

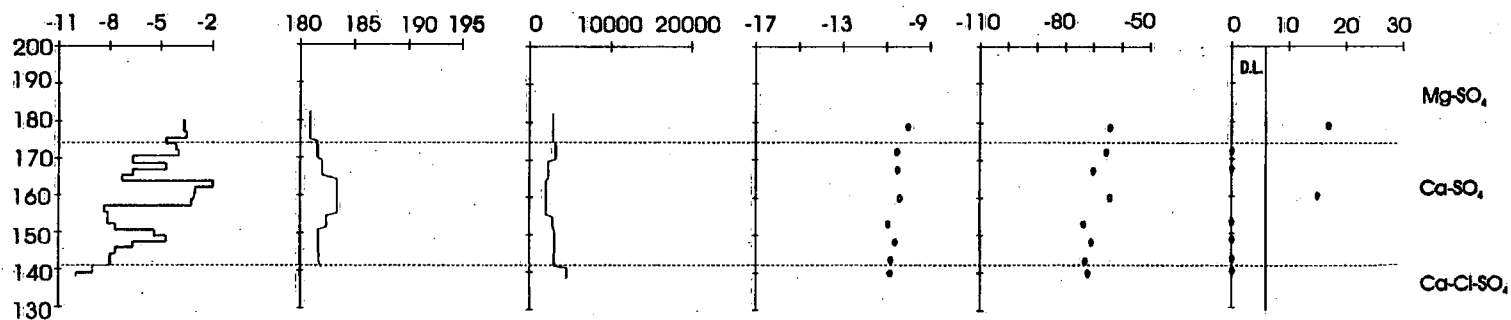


MASL

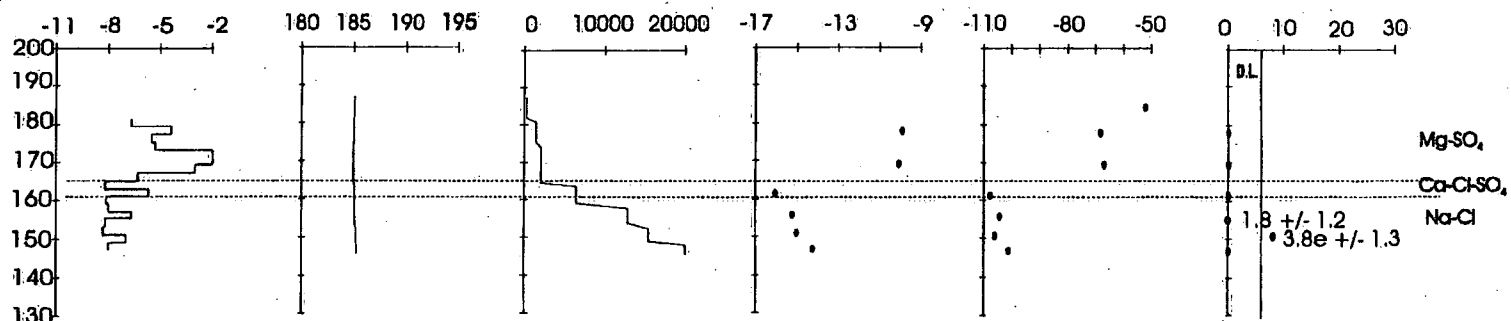
BH53



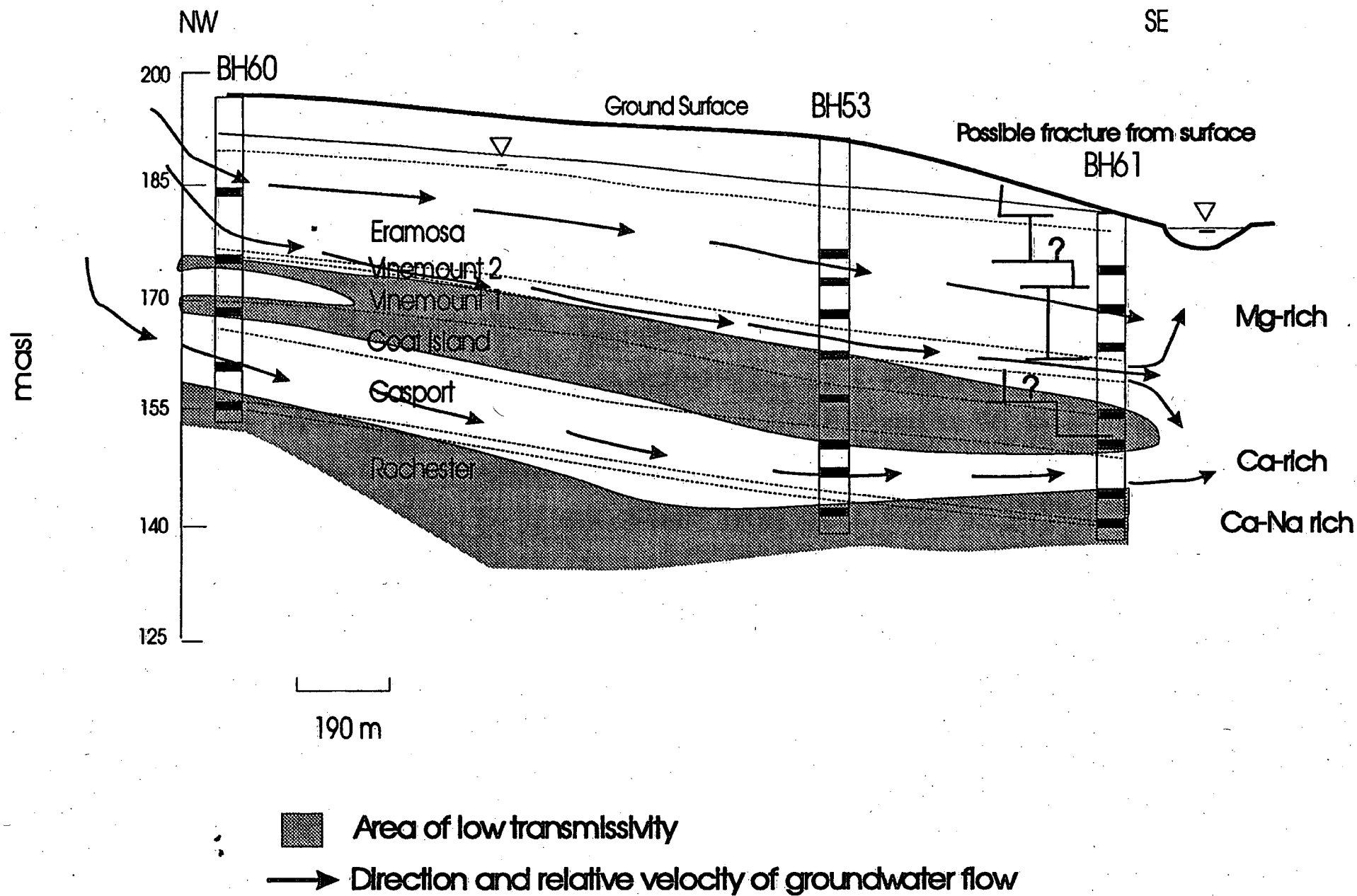
BH61



BH65



Overburden Eramosa Vinemount Goat Island Gasport Rochester



Environment Canada Library, Burlington



3 9055 1017 7225 8

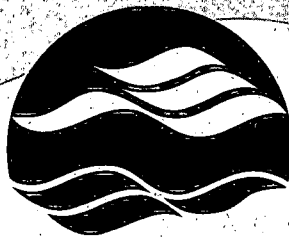
PRINTED IN CANADA
IMPRIMÉ AU CANADA



ON RECYCLED PAPER
SUR DU PAPIER RECYCLÉ

National Water Research Institute
Environment Canada
Canada Centre for Inland Waters
P.O. Box 5050
867 Lakeshore Road
Burlington, Ontario
L7R 4A6 Canada

National Hydrology Research Centre
11 Innovation Boulevard
Saskatoon, Saskatchewan
S7N 3H5 Canada



**NATIONAL WATER
RESEARCH INSTITUTE**
**INSTITUT NATIONAL DE
RECHERCHE SUR LES EAUX**

Institut national de recherche sur les eaux
Environnement Canada
Centre canadien des eaux intérieures
Case postale 5050
867, chemin Lakeshore
Burlington, Ontario
L7R 4A6 Canada

Centre national de recherche en hydrologie
11, boul. Innovation
Saskatoon, Saskatchewan
S7N 3H5 Canada



Environment · Environnement
Canada Canada

Canada